



MRI-based radiomics nomogram may predict the response to induction chemotherapy and survival in locally advanced nasopharyngeal carcinoma

Lina Zhao¹ · Jie Gong² · Yibin Xi³ · Man Xu¹ · Chen Li³ · Xiaowei Kang³ · Yutian Yin¹ · Wei Qin² · Hong Yin³ · Mei Shi¹

Received: 8 January 2019 / Revised: 21 March 2019 / Accepted: 2 April 2019 / Published online: 1 August 2019

© European Society of Radiology 2019

Abstract

Objectives To establish and validate a radiomics nomogram for prediction of induction chemotherapy (IC) response and survival in nasopharyngeal carcinoma (NPC) patients.

Methods One hundred twenty-three NPC patients (100 in training and 23 in validation cohort) with multi-MR images were enrolled. A radiomics nomogram was established by integrating the clinical data and radiomics signature generated by support vector machine.

Results The radiomics signature consisting of 19 selected features from the joint T1-weighted (T1-WI), T2-weighted (T2-WI), and contrast-enhanced T1-weighted MRI images (T1-C) showed good prognostic performance in terms of evaluating IC response in two cohorts. The radiomics nomogram established by integrating the radiomics signature with clinical data outperformed clinical nomogram alone (C-index in validation cohort, 0.863 vs 0.549; $p < 0.01$). Decision curve analysis demonstrated the clinical utility of the radiomics nomogram. Survival analysis showed that IC responders had significant better PFS (progression-free survival) than non-responders (3-year PFS 84.81% vs 39.75%, $p < 0.001$). Low-risk groups defined by radiomics signature had significant better PFS than high-risk groups (3-year PFS 76.24% vs 48.04%, $p < 0.05$).

Conclusions Multiparametric MRI-based radiomics could be helpful for personalized risk stratification and treatment in NPC patients receiving IC.

Key Points

- MRI Radiomics can predict IC response and survival in non-endemic NPC.
- Radiomics signature in combination with clinical data showed excellent predictive performance.
- Radiomics signature could separate patients into two groups with different prognosis.

Keywords Nasopharyngeal carcinoma · Magnetic resonance imaging · Radiomics · Machine learning · Induction chemotherapy

Abbreviations

CCRT Concurrent chemoradiation
IC Induction chemotherapy
IMRT Intensity-modulated radiotherapy

LASSO Least absolute shrinkage and selection operator
NPC Nasopharyngeal carcinoma
PFS Progression-free survival
RF Random forest

Lina Zhao and Jie Gong contributed equally to this work.

Electronic supplementary material The online version of this article (<https://doi.org/10.1007/s00330-019-06211-x>) contains supplementary material, which is available to authorized users.

✉ Wei Qin
wqin@xidian.edu.cn

✉ Mei Shi
mshi82@hotmail.com

² Life Sciences Research Center, School of Life Sciences and Technology, Xidian University, Xi'an 710126, China

³ Department of Radiology, Xijing Hospital, Air Force Medical University, Xi'an, China

¹ Department of Radiation Oncology, Xijing Hospital, Air Force Medical University, Xi'an, China

SVM Support vector machine
T1-C T1 contrast

Introduction

Nasopharyngeal carcinoma (NPC) is the most common head and neck cancer in Southeast Asia. Previous studies indicated that NPC had different characteristics in endemic vs non-endemic areas [1, 2]. Concurrent chemoradiation (CCRT) is a standard of care for locally advanced NPC [3]. With the development of intensity-modulated radiotherapy (IMRT), despite a favorable 5-year local rate (> 90%), distant metastases are the predominant risk [2, 4, 5], suggesting a need for more systemic therapies. Induction chemotherapy (IC) is better tolerated than adjuvant chemotherapy, and the achieved dose intensity is greater. A meta-analysis and one phase III trial both indicated that IC could improve survival compared with CCRT alone in locoregionally advanced NPC [6, 7]. We suggested that IC-CCRT was safe and effective in the treatment of NPC from non-endemic regions [8].

Tumor response to IC is an independent prognostic factor for survival after IMRT in NPC [9]. However, not all patients respond well to IC. Pretreatment identification of non-responders would allow more personalized treatment selection, avoiding toxicity and unnecessary costs for non-responders. However, no ideal clinical features or biological biomarker is available today.

Modalities like 18F-fluorodeoxyglucose positron emission tomography and MRI-DWI have been proposed as potential imaging biomarkers for the prediction of response to IC in NPC [10, 11]. Radiomic analysis is promising in cancer diagnosis, prognosis, and prediction of response to treatment [12, 13]. Recent studies showed that texture parameter of pretreatment MRI or MRI-based radiomics nomogram could predict PFS in endemic NPC [14, 15]. Pretreatment MRI signature could also predict early IC response in endemic NPC patients, although there was no independent validation [16]. However, no study has reported the role of MRI-based radiomics for the prediction of IC response in non-endemic region. Its role in predicting both IC response and survival is still unclear. The current study aims to investigate the role of a MRI-based radiomics nomogram in predicting the response to IC in locally advanced NPC patients of Northwest China. Also, we sought to correlate it with clinical parameters and survival.

Materials and methods

Patients

A total of 200 patients with histologically confirmed NPC treated with IC and CCRT between January 2012 and December 2016 in Xijing Hospital were enrolled in the study. T1-WI, T2-WI, and T1-C (T1 contrast) images were collected before treatment (3-T GE or Siemens MRI scanners). All patients were staged according to the 7th Edition of American Joint Committee on Cancer (AJCC) TNM classification. A total of 123 patients were enrolled and were allocated to the training and validation cohorts randomly. One hundred and 23 patients were allocated to the training cohort (28 responders vs 72 non-responders) and validation cohort (6 responders vs 17 non-responders), respectively. The details of chemotherapy are shown in [supplemental materials](#).

Endpoints and follow-up

The clinical treatment response after IC was defined as stable disease (SD), progressive disease (PD), partial response (PR), or complete response (CR) based on the Response Evaluation Criteria in Solid Tumors 1.1 (RECIST) criteria [17]. Patients were categorized into IC responders (CR/PR) and non-responders (SD/PD). All patients were followed up weekly during radiotherapy treatment and every 2–3 months during the first 2 years, then every 3–4 months during the year after radiotherapy treatment 3–5, and annually thereafter.

Tumor segmentation, radiomics feature extraction, and development of multiparametric MRI-based radiomics model

The details of tumor segmentation (Fig. 1a) are shown in [supplemental methods](#). Imaging features calculated for each patient from a unimodal MR image using MATLAB procedure algorithm (Fig. 1b), which was described in the [supplemental material](#). Features from T1-C, T1-WI, and T2-WI or the combination were used for subsequent analysis, respectively. For the feature selection step, a filter method based on the selection frequency was employed to obtain a ranking of features with the most discriminative power. The frequency of each feature selected by the two-step feature selection methods across 100 training partitions of the leave-one-out cross-validation (LOOCV) was calculated to assess the variable importance (> 50% selection probability across partitions). The two-step feature selection method consisted the two-sample *t* test between responders and non-responder in the training cohort and the logistic regression model with

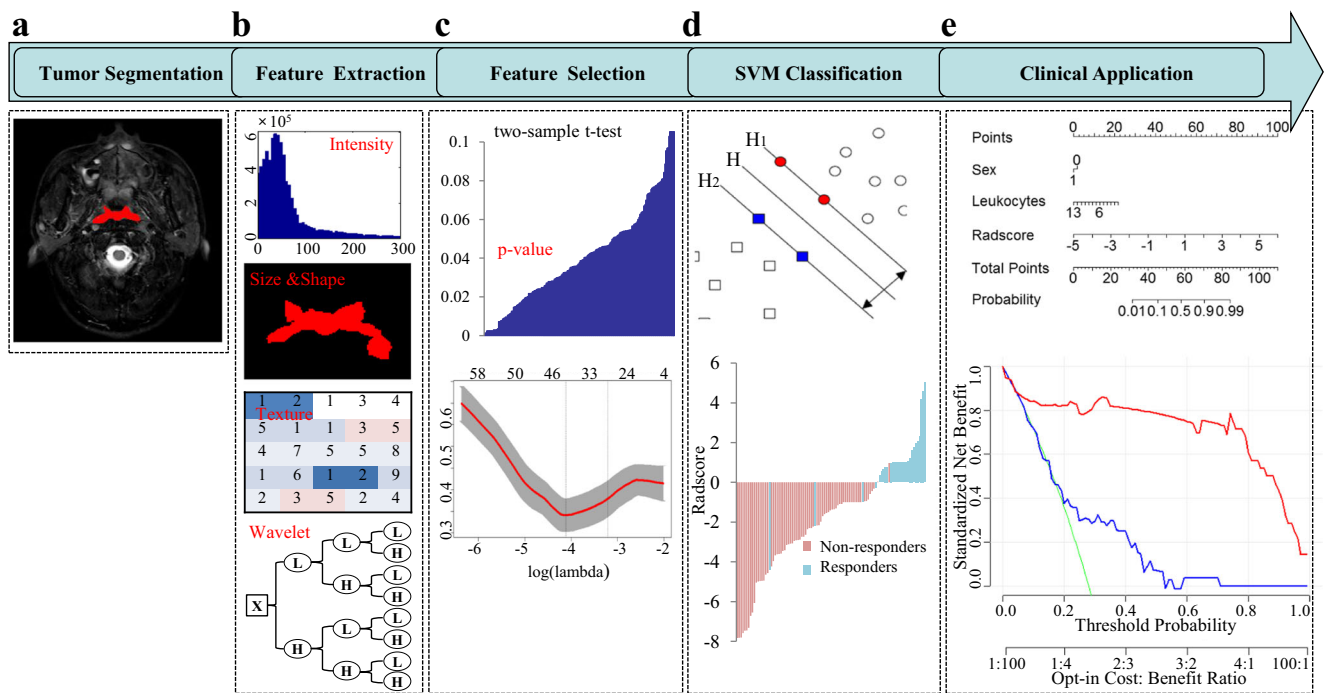


Fig. 1 A general schema for predictive nomogram establishment. **a** Three-dimensional manual segmentation. **b** Four types of features were finally calculated for each patient from single segmentation. **c** The two-sample *t* test and the logistic regression model with LASSO

based on LOOCV were used to select useful features. **d** Radiomics signature was established with support vector machine. **e** Multivariable backward stepwise logistic regression model was used to develop a radiomics nomogram

LASSO (the least absolute shrinkage and selection operator) (Fig. 1c) [18–20]. A tuning parameter λ which controls the strength of regularization was chosen using tenfold cross-validation repeated 1000 times via minimum criteria. All important features were ranked by the selection frequency.

The ranked 29 features (> 50% selection probability) were used to generate different subsets and train the SVM (support vector machine) model. For example, the first subset consisted of the first two features, the second one consisted of the first three features, and so on. Twenty-eight feature subsets were generated in total. The support vector machine (SVM) with linear kernel was developed to evaluate the role of each feature subset in predicting the response to IC (Fig. 1d). Tenfold cross-validation was applied to select the regularization parameter *C* from 0.01 to 1 with a step size 0.01 based on AUC maximum criteria. In this study, fivefold cross-validation was used to estimate group classification and prediction accuracies and repeated 1000 times in the training cohort. Furthermore, the feature subset with the best performance was used to train and validate the final SVM model in the training and validation cohort respectively. The optimal cutoff value of the radscore were based on the score test from the Cox regression model and calculated from the “cutp” function of the “survMisc” R package [21]. Random forest (RF) was used as a second machine learning algorithm to validate the previous results (supplemental methods).

Accuracy (ACC), positive predictive value (PPV), negative predictive value (NPV), and the area under the receiver operating characteristic curve (AUC) are used for evaluating the model performance. ROC curves were drawn to display and compare the performance of different models [22]. Identification of the role of radiomics signature in the prediction of survival is shown in supplemental materials.

Development of the clinical and radiomics nomogram

Multivariable logistic regression model-based nomograms are shown in Fig. 1e. The clinical parameters used in the clinical model include the following: age; gender; T, N, and clinical stage; EB-DNA; histology; IC cycles and regimens; the diameter and volume of lymph nodes and nasopharyngeal before IC; and the level of leukocytes, platelets, lymphocytes, and albumin before IC. Radscore from the joint multimodal images was enrolled in the establishment of radiomics nomogram. The likelihood ratio test with Akaike’s information criterion was applied as the stopping rule for backward stepwise logistic regression analysis. Harrell’s C-index, AUC, ACC, PPV, and NPV were used to quantify the discriminative performance. Decision curve analysis was conducted to estimate the clinical usefulness of the models. The details of statistical analysis are described in the supplemental material.

Table 1 Characteristics of the patients in the training and validation cohorts (χ^2 test)

Parameters	Training			Validation		
	Responders (<i>n</i> = 28)	Non-responders (<i>n</i> = 72)	<i>p</i>	Responders (<i>n</i> = 6)	Non-responders (<i>n</i> = 17)	<i>p</i>
Age (years) ^b			0.581			0.131
Mean ± SD	49.43 ± 11.55	48.13 ± 10.18		52.17 ± 5.12	44.76 ± 10.99	
Sex			0.024			0.423
Male	4 (14.3)	27 (37.5)		2 (33.3)	3 (17.6)	
Female	24 (85.7)	45 (62.5)		4 (66.7)	14 (82.4)	
AJCC			0.746			0.131
T1	2 (7.1)	4 (5.6)		0 (0)	2 (11.8)	
T2	9 (32.1)	22 (30.6)		0 (0)	3 (17.6)	
T3	8 (28.6)	15 (20.8)		3 (50.0)	2 (11.8)	
T4	9 (32.1)	31 (43.1)		3 (50.0)	10 (58.8)	
AJCC			0.083			0.613
N0	0 (0)	1 (1.4)		0 (0)	0 (0)	
N1	5 (17.9)	4 (5.6)		2 (33.3)	3 (17.6)	
N2	10 (35.7)	43 (59.7)		3 (50.0)	10 (58.8)	
N3	5 (17.9)	14 (19.4)		1 (16.7)	2 (11.8)	
N4	8 (28.6)	10 (13.9)		0 (0)	2 (11.8)	
Clinical stage			0.475			0.669
III	8 (28.6)	25 (34.7)		3 (50.0)	5 (29.4)	
IVa	7 (25.0)	23 (31.9)		2 (33.3)	8 (47.1)	
IVb	13 (46.4)	24 (33.3)		1 (16.7)	4 (23.5)	
EB-DNA			0.040			0.462
< 5000 copies/ml	25 (89.2)	50 (69.4)		5 (83.3)	16 (94.2)	
≥ 5000 copies/ml	3 (10.7)	22 (30.6)		1 (16.7)	1 (5.9)	
Histology			0.937			1.000
WHO II	8 (28.6)	20 (27.8)		1 (16.7)	5 (29.4)	
WHO III	20 (71.4)	52 (72.2)		5 (83.3)	12 (70.6)	
Induction chemotherapy regimens			0.340			0.462
TP	21 (75.0)	60 (83.3)		5 (83.3)	16 (94.1)	
GP	7 (25.0)	12 (16.7)		1 (16.7)	1 (5.9)	
White blood cells ^b			0.148			0.736
Mean ± SD	6.38 ± 1.85	7.02 ± 2.00		6.34 ± 1.96	6.63 ± 1.74	
Radscore ^{cc}			< 0.001			0.006
Median (<i>Q</i> _L , <i>Q</i> _U)	1.00 (0.67, 1.73)	-2.50 (-4.17, -1.02)		0.57 (-0.97, 4.40)	-2.33 (-3.79, -0.76)	

^b Two independent sample *t* test

^{cc} Rank sum test

Results

Clinical characteristics of the patients

The characteristics of all NPC patients in both the training and validation cohorts are shown in Table 1 and Supplemental Table 1. There was no significant difference between the two cohorts in terms of IC response rate (28% and 26.1% in the training and validation cohorts, respectively, $p = 0.853$). Also, no significant difference was observed between IC responders and non-responders, except that there were more females and

more patients with ≥ 5000 copies/ml EBV DNA level in the responders group of the training cohort.

Establishment of multiparametric MRI-based radiomics signature

A total of 4503 imaging features were finally calculated for each patient from the extracted tumor region of a unimodal MR image. Twenty-nine features ($> 50\%$ selection probability) selected from the combination of the three modalities were ranked by the selection frequency and the top 19 features

Table 2 Radiomics feature selection results

Index	Name	Sequences	Category	Frequency
1	“W8.Co_Var_2”	T1-C	Textural	92
2	“W5.Cluster_Shade_2”	T1-WI	Textural	92
3	“W6.Co_Corr_mean”	T1-WI	Textural	92
4	“W5.Co_Corr_4”	T2-WI	Textural	92
5	“W8.Co_Corr_3”	T2-WI	Textural	92
6	“W3.Co_Var_9”	T2-WI	Textural	91
7	“W7.SRHGLE_3”	T1-WI	Textural	87
8	“W7.Co_Corr_9”	T2-WI	Textural	87
9	“W7.Co_Corr_4”	T2-WI	Textural	81
10	“W7.IMC1_6”	T2-WI	Textural	80
11	“W1.SRE_3”	T1-C	Textural	74
12	“W4.Cluster_Shade_2”	T1-C	Textural	74
13	“W6.IMC2_5”	T1-C	Textural	72
14	“W7.HGLRE_3”	T1-WI	Textural	71
15	“W6.SRHGLE_1”	T2-WI	Textural	66
16	“W4.Co_Corr_3”	T1-C	Textural	62
17	“W6.AutoCorr_3”	T2-WI	Textural	62
18	“W4.Min”	T2-WI	First-order	61
19	“W4.SRHGLE_11”	T2-WI	Textural	61
20	“W5.Co_Corr_3”	T1-C	Textural	55
21	“W5.LRLGLE_3”	T1-C	Textural	55
22	“W5.IDNM_3”	T1-C	Textural	54
23	“W4.SRLGLE_6”	T1-WI	Textural	52
24	“W8.IDNM_12”	T2-WI	Textural	52
25	“W1.LRE_3”	T1-C	Textural	52
26	“W7.Co_Corr_10”	T2-WI	Textural	51
27	“W7.Co_Corr_5”	T2-WI	Textural	51
28	“W7.Inverse_var_3”	T2-WI	Textural	50
29	“W8.Co_Corr_12”	T2-WI	Textural	50

Co_Var, variance; *Cluster_Shade*, cluster shade; *SRHGLE*, short run high gray level emphasis; *IMC*, Informational measure of correlation; *SRE*, short run emphasis; *HGLRE*, high gray level run emphasis; *AutoCorr*, autocorrelation; *Min*, minimum; *LRLGLE*, long run low gray level emphasis; *IDNM*, inverse difference moment normalized; *SRLGLE*, short run low gray level emphasis; *LRE*, long run emphasis; *Inverse_var*, inverse variance; *W1-8*, wavelet decompositions, *W0* represents the originate plane and *W1-8* represent 8 wavelet planes. The number written after the feature named as 1–13 represents the direction of the texture matrix. Mean indicates the average of the 13 directions

consisting of 5 from enhanced T1-C, 4 from T1-WI, and 10 from T2-WI images showed the best performance in training the models (Table 2, Fig. 2). The classification accuracy and the AUC value using the combination of three modalities by repeated fivefold cross-validation were 88.58% and 0.8866, respectively (Supplemental Table 3). Multi-modality images showed better prediction performance than unimodal MR image alone (Supplemental Table 3) and RF model generated similar results to SVM model (Supplemental Table 7). The

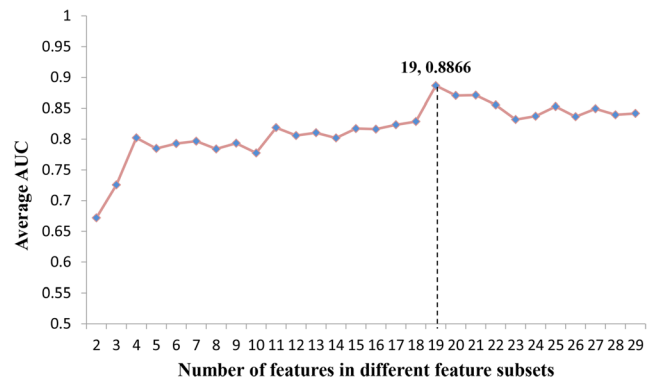


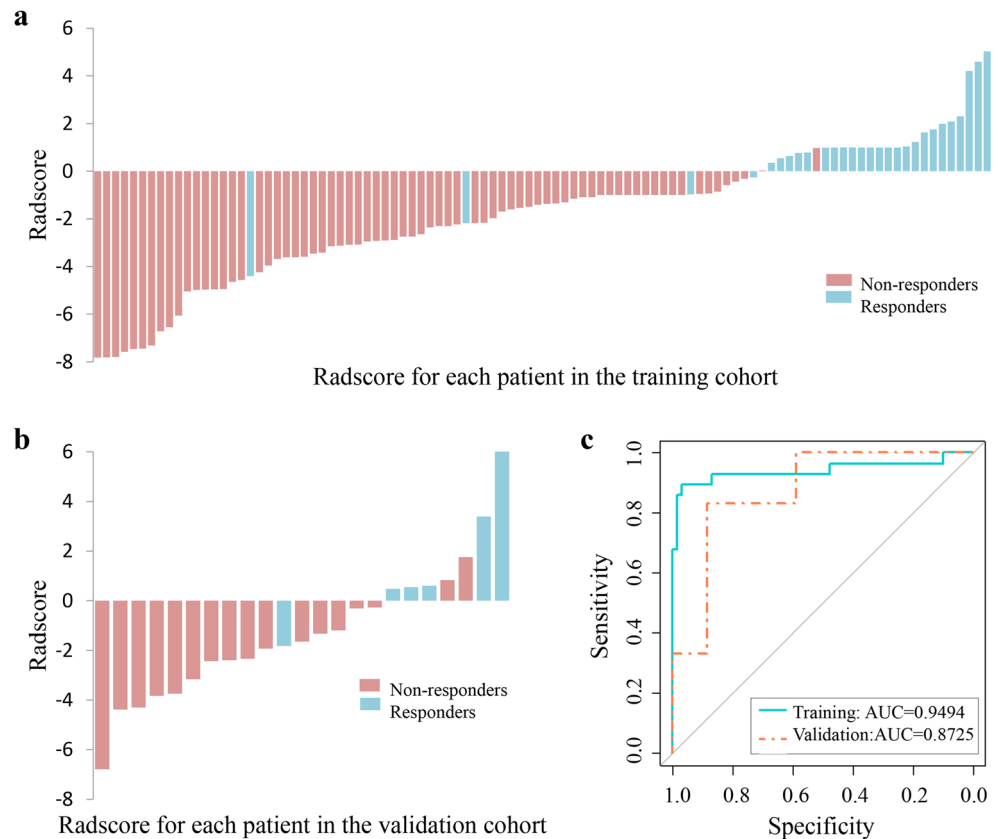
Fig. 2 One thousand times of fivefold cross-validation were used to examine different subsets of features and evaluate the SVM models. Features of the feature subset with the highest AUC value were the most important and the feature subset was used to train and validate the final SVM model in the training and validation cohort respectively

distributions of radiomics signatures for each patient in both the training and validation cohorts are shown in Fig. 3 a and b. There was a significant difference in radiomics scores between responders and non-responders in both the training cohort ($p < 0.001$) and the validation cohort ($p = 0.002$; Table 1). The AUC, ACC, PPV, and NPV of the SVM model in the training cohort were 0.9494, 95.00%, 96.00%, and 94.67%, respectively, and in the validation cohort were 0.8725, 86.96%, 71.43%, and 93.75%, respectively (Table 3). ROC curve is shown in Fig. 3c.

Establishment of clinical and radiomics nomogram

Sex and the level of leukocytes before treatment were identified as independent predictors with significance for IC response ($p < 0.05$). The clinical nomogram based on these two factors yielded a C-index of 0.708 (95% CI, 0.588–0.827) in the training cohort and 0.549 (95% CI, 0.197–0.705) in the validation cohort. The AUC, ACC, PPV, and NPV of clinical nomogram in the training cohort were 0.7076, 76%, 62.50%, and 78.57%, respectively, and in the validation cohort were 0.5490, 65.22%, 0%, and 71.43%, respectively (Table 3). ROC curve is shown in Fig. 4a. We next developed a radiomics nomogram that integrated the radiomics signature ($p < 0.0001$) from the joint T1-C, T1-WI, and T2-WI with all the independent clinical factors, which provided a higher C-index of 0.952 (95% CI, 0.895–1) in the training cohort and 0.863 (95%CI: 0.706–1) in the validation cohort (Fig. 4c). The AUC, ACC, PPV, and NPV of the radiomics nomogram in the training cohort were 0.9524, 95.00%, 92.59%, and 95.89%, respectively, and in the validation cohort were 0.8627, 82.61%, 100%, and 80.95%, respectively (Table 3). The ROC curves are shown in Fig. 4b. The calibration curves of the radiomics nomogram showed good agreement between the observed actual probabilities of the response and nomogram predicted probabilities in the training

Fig. 3 The distribution of radiomics signature and performance of the SVM model. **a** Distributions of radiomics signature in the training cohort. **b** Distributions of radiomics signature in the validation cohort. **c** ROC curves for the SVM model in the training and validation cohorts



and validation cohorts shown in Fig. 5 a and b, respectively. The decision curve analysis for the radiomics nomogram is presented in Fig. 5c, showing that the radiomics nomogram provided better performance.

The role of radiomics signature in the prediction of survival

Survival analysis showed that responders to IC had significantly better PFS than non-responders (3-year PFS 84.81% vs 39.75%, $p < 0.001$; Fig. 6a). Log-rank test was used to select the radscore with significant significance and radscore value (-0.317) was used to divide patients into high- and low-risk groups for different PFS. Low-risk groups with higher

radiomics signature had significantly better PFS than higher-risk groups (3-year PFS 76.24% vs 48.04%, $p < 0.05$; Fig. 6b).

Discussion

In this study, we established a multiparametric MRI-based radiomics nomogram to predict IC response before treatment in locally advanced non-endemic NPC. The radiomics signatures from combination of T1-WI, T2-WI, and enhanced T1-WI images demonstrated excellent prediction value. The nomogram established by addition of MRI radiomics to clinical parameters outperformed that based on clinical data alone. Also, the radiomics signature could separate patients into

Table 3 Performance of SVM classification, clinical model, and radiomics-based nomogram

Metrics	Radiomics signature		Clinical model		Radiomics-based nomogram	
	Primary cohort	Validation cohort	Primary cohort	Validation cohort	Primary cohort	Validation cohort
AUC	0.9494	0.8725	0.7076	0.5490	0.9524	0.8627
ACC	95.00%	86.96%	76.00%	65.22%	95.00%	82.61%
PPV	96.00%	71.43%	62.50%	0.00%	92.59%	100.00%
NPV	94.67%	93.75%	78.57%	71.43%	95.89%	80.95%

AUC, the area under ROC curve; ACC, accuracy; PPV, positive predictive value; NPV, negative predictive value

Fig. 4 The radiomics nomogram and the ROC curves in both the training and validation cohorts. **a** ROC curves for the clinical nomogram in the training and validation cohorts. **b** ROC curves for the radiomics nomogram in the training and validation cohorts. **c** Radiomics nomogram integrating the radiomics signature from the joint T1-C, T1-W, and T2-W with all the independent clinical factors. **d** Representative T2-WI image of NPC patient as IC responder before and after IC. **e** Representative T2-WI image of NPC patient as IC non-responder before and after IC

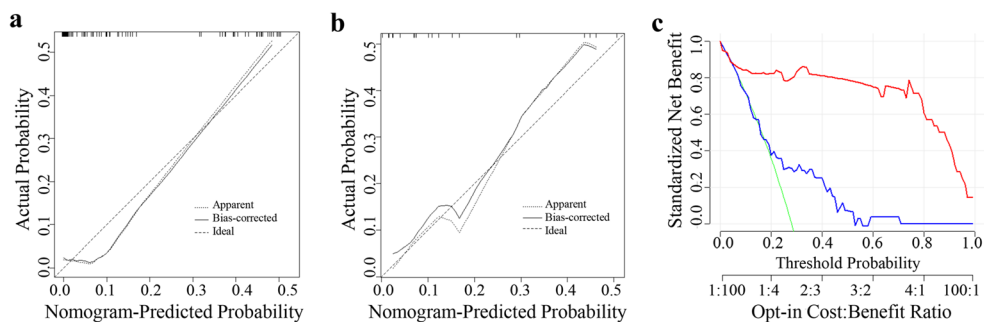
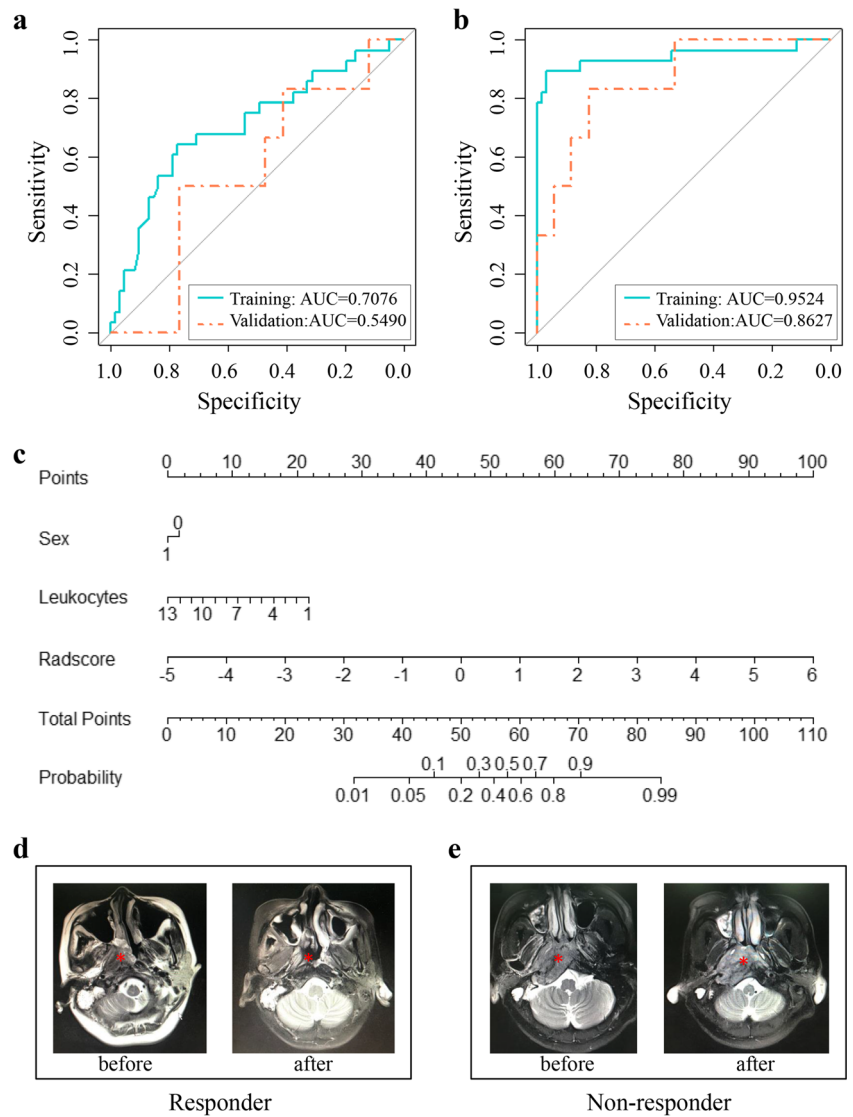
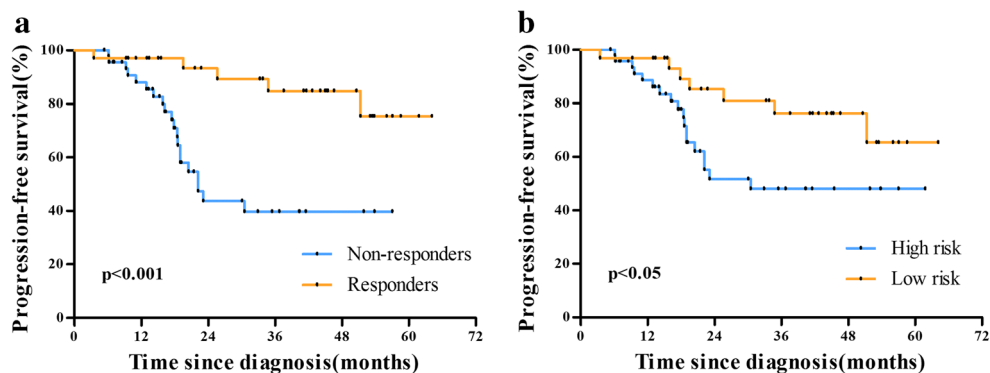


Fig. 5 The calibration and decision curves. **a** Calibration curves for the radiomics nomogram in the training cohort. The dashed line indicated ideal reference line where predicted probabilities would match the observed proportions. The solid line represented the performance of the radiomics nomogram. **b** Calibration curves for the radiomics nomogram in the validation cohort. **c** Decision curve analysis for the radiomics

nomogram. The x-axis represented the probability of the response to IC ranging from 0 to 100%. The y-axis measured the net benefit. The black line represented the scheme in which all patients were assumed to be responders. The gray line represented the assumption that all patients were non-responders

Fig. 6 Survival analysis stratified by IC response and radiomics signature. **a** Survival analysis for responders and non-responders to IC. **b** Survival analysis for high- and low-risk patients with different radiomics signatures



high- and low-risk groups based on significantly different PFS rate.

Anatomical MRI has been widely used to determine the treatment response in NPC [23]. Currently, there are no ideal clinical features or biomarkers to predict IC response in NPC. One study found NPC patients with low ADCs before treatment responded better to IC [10]. In a retrospective study consisting of 120 endemic NPC patients, pretreatment MRI radiomics signature could predict early IC response [16]. However, there was no validation by an independent cohort. One study showed that MRI-based texture analysis had the potential to predict chemoradiotherapy response with a high accuracy, but this was in a relatively small number of NPC patients [24]. In another study, T2-weighted and contrast-enhanced T1-weighted MRI radiomics predicted progression of endemic NPC in both the training and validation groups [25].

However, several key points need to be considered in MRI radiomics prediction model establishment. Firstly, the majority of MRI radiomics studies were performed in endemic NPC patients and the predictive model cannot be directly applied to non-endemic NPC, given that characteristics differentiate endemic and non-endemic tumors. Our previous studies indicated that WHO type II histology represented a higher proportion of cases diagnosed in northwest China versus endemic regions ($> 25\%$ vs $< 10\%$) and WHO type II histology was associated with poor outcomes. Furthermore, less than 15% patients had detectable EBV DNA, while over 90% patients in endemic regions have detectable EBV DNA [1, 2]. Here, we established and validated a radiomics nomogram for non-endemic NPC patients and more studies need to be done to study the difference of radiomics between endemic and non-endemic NPC.

Secondly, the role of clinical factors or the combination of clinical factors and radiomics needs to be clarified. One recent study extracted 970 radiomics features from T2-WI and contrast-enhanced T1-WI MRI [15]. The radiomics nomogram was established by combining radiomics signature with TNM and showed a significant improvement in PFS prediction of NPC when compared with TNM alone. Our study

developed a radiomics nomogram that integrated radiomics signature from the joint T1-C, T1-WI, and T2-WI with all the independent clinical factors. This provided a higher C-index in both the training and validation cohorts, indicating that radiomics was more accurate than the clinical nomogram alone in the prediction of IC response. Accordingly, radiomics features seems to be more sensitively and closely correlated with the clinical endpoints we defined (clinical treatment response after IC was the endpoint in this study) when compared with diagnostic radiologic, or clinical information.

Lastly, the role of multiple versus single MRI sequences needs to be studied. Here, we used three MRI sequences to extract image radiomics features, and 4503 imaging features were calculated for each patient from single modality. Of these, 19 features consisting of 5 from enhanced T1-C, 4 from T1-WI, 10 from T2-WI images were input to the SVM model. Our results showed that features extracted from several sequences performed better than when acquired from a single sequence, as shown by both fivefold cross-validation in the training cohort and independent validation in the validation cohort. In order to overcome the limitation of SVM, we also used the random forest (RF) as a second machine learning algorithm and the results were similar. Image information from different sequences could be a more meaningful representation of the radiomics diversity within the tumor.

Given the capability to predict IC response in NPC, we wondered whether this model could also predict survival, which is a very important clinical endpoint. Some reports have showed that tumor response to IC was an independent prognostic factor for survival after radiation therapy in NPC [9]. In this study, we also found that IC responders had significantly better PFS than those non-responders (3-year PFS 84.81% vs 39.75%, $p < 0.001$). Also, we divided patients into high-risk and low-risk groups by radiomics signature. The low-risk group had a significantly better PFS. These results were in accordance with a previous study showing a significant improvement in PFS prediction by combination of radiomics and TNM than by TNM alone [15].

It has long been demonstrated that radiomics features were associated with tumor biology. Adding radiomics features to

molecular pathology is an important extension of radiomics [13]. Panth KM et al found radiomics was able to identify early effects of changed gene expression after radiation treatment in tumors with similar volumes [26]. “Radio-genomics” combining radiomics with genomics data is another emerging prognostic tool [13]. One study indicated that neuroimaging and DNA microarray analysis could create a multidimensional map of gene expression patterns in glioblastoma multiforme [27]. Another study indicated that measures of spatial diversity from MRI images were associated with both tumor subtype status and survival status [28]. In NLCLC, a study established a radiogenomics map and found a metagene from EGF pathway was significantly correlated with ground-glass opacity and irregular nodules or nodules with poorly defined margins [29]. NRG Oncology HN001 trial (NCT02135042) is ongoing with the aim to identify NPC patients who would more likely benefit from additional systemic chemotherapy based on EBV DNA levels. Therefore, radiogenomics in prediction of NPC treatment response and prognosis is an attractive future direction.

Because of its retrospective nature, our study has several limitations. Firstly, due to the critical inclusion criteria of patients included, we had a relatively small number of patients that may affect the final conclusion of the study. Secondly, the single institutional nature of the study may also limit the applicability of our findings for patients from other geographical regions and institutions. Lastly, as pathologic examination of the treatment response was not possible in NPC patients who are mainly treated by radiotherapy, IC response evaluation only based on anatomical MRI imaging might be less accurate. Furthermore, other MRI technique, especially DCE-MRI-based radiomics, has been used in the prediction of treatment response for breast cancer and its role in NPC needs to be further explored [30].

In conclusion, the current study established a multiparametric MRI-based radiomics nomogram to predict the IC response before treatment in locally advanced NPC in non-endemic areas. The results might be more easily generalizable in other countries, due to the non-endemic nature of this cohort. MRI-based radiomics could be especially helpful for personalized risk stratification and treatment in NPC patients receiving IC.

Funding This study has received funding by the National Natural Science Foundation of China Grants 81872699 and Key project of Shanxi Province 2017ZDXM-SF-043.

Compliance with ethical standards

Guarantor The scientific guarantor of this publication is Lina Zhao.

Conflict of interest The authors of this manuscript declare no relationships with any companies, whose products or services may be related to the subject matter of the article.

Statistics and biometry Yutian Yin, one of the authors, has significant statistical expertise.

Informed consent Written informed consent was not required for this study because the retrospective nature of the study.

Ethical approval Institutional Review Board approval was obtained.

Methodology

- retrospective
- diagnostic or prognostic study
- performed at one institution

References

1. Zang J, Li C, Zhao LN et al (2016) Prognostic model of death and distant metastasis for nasopharyngeal carcinoma patients receiving 3DCRT/IMRT in nonendemic area of China. *Medicine (Baltimore)* 95:e3794
2. Zhao LN, Zhou B, Shi M et al (2012) Clinical outcome for nasopharyngeal carcinoma with predominantly WHO II histology treated with intensity-modulated radiation therapy in non-endemic region of China. *Oral Oncol* 48:864–869
3. Al-Sarraf M, LeBlanc M, Giri PG et al (1998) Chemoradiotherapy versus radiotherapy in patients with advanced nasopharyngeal cancer: phase III randomized intergroup study 0099. *J Clin Oncol* 16: 1310–1317
4. Wang J, Shi M, Hsia Y et al (2012) Failure patterns and survival in patients with nasopharyngeal carcinoma treated with intensity modulated radiation in Northwest China: a pilot study. *Radiat Oncol* 7:2
5. Wee CW, Keam B, Heo DS, Sung MW, Won TB, Wu HG (2015) Locoregionally advanced nasopharyngeal carcinoma treated with intensity-modulated radiotherapy plus concurrent weekly cisplatin with or without neoadjuvant chemotherapy. *Radiat Oncol J* 33:98–108
6. Blanchard P, Lee A, Marguet S et al (2015) Chemotherapy and radiotherapy in nasopharyngeal carcinoma: an update of the MAC-NPC meta-analysis. *Lancet Oncol* 16:645–655
7. Cao SM, Yang Q, Guo L et al (2017) Neoadjuvant chemotherapy followed by concurrent chemoradiotherapy versus concurrent chemoradiotherapy alone in locoregionally advanced nasopharyngeal carcinoma: a phase III multicentre randomised controlled trial. *Eur J Cancer* 75:14–23
8. Zhao L, Xu M, Jiang W et al (2017) Induction chemotherapy for the treatment of non-endemic locally advanced nasopharyngeal carcinoma. *Oncotarget* 8:6763–6774
9. Peng H, Chen L, Zhang Y et al (2016) The tumour response to induction chemotherapy has prognostic value for long-term survival outcomes after intensity-modulated radiation therapy in nasopharyngeal carcinoma. *Sci Rep* 6:24835
10. Zhang GY, Wang YJ, Liu JP et al (2015) Pretreatment diffusion-weighted MRI can predict the response to neoadjuvant chemotherapy in patients with nasopharyngeal carcinoma. *Biomed Res Int* 2015:307943
11. Yen RF, Chen TH, Ting LL, Tzen KY, Pan MH, Hong RL (2005) Early restaging whole-body (18)F-FDG PET during induction chemotherapy predicts clinical outcome in patients with locoregionally advanced nasopharyngeal carcinoma. *Eur J Nucl Med Mol Imaging* 32:1152–1159
12. Gillies RJ, Kinahan PE, Hricak H (2016) Radiomics: images are more than pictures, they are data. *Radiology* 278:563–577

13. Verma V, Simone CB 2nd, Krishnan S, Lin SH, Yang J, Hahn SM (2017) The rise of radiomics and implications for oncologic management. *J Natl Cancer Inst* 109
14. Mao J, Fang J, Duan X et al (2019) Predictive value of pretreatment MRI texture analysis in patients with primary nasopharyngeal carcinoma. *Eur Radiol*. <https://doi.org/10.1007/s00330-018-5961-6>
15. Zhang B, Tian J, Dong D et al (2017) Radiomics features of multiparametric MRI as novel prognostic factors in advanced nasopharyngeal carcinoma. *Clin Cancer Res*. <https://doi.org/10.1158/1078-0432.CCR-16-2910>
16. Wang G, He L, Yuan C, Huang Y, Liu Z, Liang C (2018) Pretreatment MR imaging radiomics signatures for response prediction to induction chemotherapy in patients with nasopharyngeal carcinoma. *Eur J Radiol* 98:100–106
17. Eisenhauer EA, Therasse P, Bogaerts J et al (2009) New response evaluation criteria in solid tumours: revised RECIST guideline (version 1.1). *Eur J Cancer* 45:228–247
18. Sauerbrei W, Royston P, Binder H (2007) Selection of important variables and determination of functional form for continuous predictors in multivariable model building. *Stat Med* 26:5512–5528
19. Smyser CD, Dosenbach NU, Smyser TA et al (2016) Prediction of brain maturity in infants using machine-learning algorithms. *Neuroimage* 136:1–9
20. Liu Z, Zhang XY, Shi YJ et al (2017) Radiomics analysis for evaluation of pathological complete response to neoadjuvant chemoradiotherapy in locally advanced rectal cancer. *Clin Cancer Res* 23:7253–7262
21. Contal COQJ (1999) An application of changepoint methods in studying the effect of age on survival in breast cancer. *Comput Stat Data Anal* 30:253–270
22. Cui Z, Xia Z, Su M, Shu H, Gong G (2016) Disrupted white matter connectivity underlying developmental dyslexia: a machine learning approach. *Hum Brain Mapp* 37:1443–1458
23. Liao XB, Mao YP, Liu LZ et al (2008) How does magnetic resonance imaging influence staging according to AJCC staging system for nasopharyngeal carcinoma compared with computed tomography? *Int J Radiat Oncol Biol Phys* 72:1368–1377
24. Liu J, Mao Y, Li Z et al (2016) Use of texture analysis based on contrast-enhanced MRI to predict treatment response to chemoradiotherapy in nasopharyngeal carcinoma. *J Magn Reson Imaging* 44:445–455
25. Zhang B, Ouyang F, Gu D et al (2017) Advanced nasopharyngeal carcinoma: pre-treatment prediction of progression based on multiparametric MRI radiomics. *Oncotarget* 8:72457–72465
26. Panth KM, Leijenaar RT, Carvalho S et al (2015) Is there a causal relationship between genetic changes and radiomics-based image features? An in vivo preclinical experiment with doxycycline inducible GADD34 tumor cells. *Radiother Oncol* 116:462–466
27. Diehn M, Nardini C, Wang DS et al (2008) Identification of non-invasive imaging surrogates for brain tumor gene-expression modules. *Proc Natl Acad Sci U S A* 105:5213–5218
28. Lee J, Narang S, Martinez J, Rao G, Rao A (2015) Spatial habitat features derived from multiparametric magnetic resonance imaging data are associated with molecular subtype and 12-month survival status in glioblastoma multiforme. *PLoS One* 10:e0136557
29. Zhou M, Leung A, Echegaray S et al (2017) Non-small cell lung cancer radiogenomics map identifies relationships between molecular and imaging phenotypes with prognostic implications. *Radiology*. <https://doi.org/10.1148/radiol.2017161845:161845>
30. Mani S, Chen Y, Li X et al (2013) Machine learning for predicting the response of breast cancer to neoadjuvant chemotherapy. *J Am Med Inform Assoc* 20:688–695

Publisher's note Springer Nature remains neutral with regard to jurisdictional claims in published maps and institutional affiliations.